International Journal of Mechanical and Production Engineering Research and Development (IJMPERD)
ISSN(P): 2249-6890; ISSN(E): 2249-8001
Vol. 9, Issue 2, Apr 2019, 903-920

STUDIES ON MILD STEEL PARTICULATES REINFORCED DURALUMIN COMPOSITE FABRICATED THROUGH POWDER METALLURGY ROUTE

Y. M SHIVAPRAKASH[1], B. M. GURUMURTHY[2*], M. A. SIDDHARTHA[3], N. M. SIDDESH KUMAR[3] & AVISHEK DUTTA[3]

[1]*Associate Professor, Department of Mechanical and Manufacturing Engineering, Manipal Institute of Technology, Manipal Academy of Higher Education, Manipal, Karnataka, India*

[2]*Assistant Professor, Department of Mechanical and Manufacturing Engineering, Manipal Institute of Technology, Manipal Academy of Higher Education, Manipal, Karnataka, India*

[3]*Student, Department of Mechanical and Manufacturing Engineering, Manipal Institute of Technology, Manipal Academy of Higher Education, Manipal, Karnataka, India*

ABSTRACT

In the present study Duralumin(DA) based Mild Steel particles (MS_p-6% wt. and 12% wt.) reinforced composite are fabricated by cold compacting the milled powders. The mechanically mixed powders are compacted in a die cavity by applying a uniaxial steady load in the range 22-38 T. The hardness of green compacts produced are increased by sintering. The SEM images showed an even dispersion of MS_p in the duralumin alloy and elemental composition is confirmed by the EDAX spectrum. The sintered specimens were further subjected to aging treatment. Compacts were soaked at 550^{0}C for a span of 2 h and then are quenched in water at ambient temperature. The temperatures selected for aging treatment are 100, 150, and 200^{0}C and hardness was checked for every 60 minutes of time. The peak hardness obtained because of aging heat treatment is found to be much better than the corresponding sintered compacts. Compacts peak aged at 100^{0}C exhibited better tensile strength than the rest of the other specimens.

KEYWORDS: Duralumin, Mild Steel Powder, Ball Milling, Cold Compacting & Aging Treatment

Received: Feb 17, 2019; **Accepted:** Mar 07, 2019; **Published:** Apr 05, 2019; **Paper Id.:** IJMPERDAPR201988

Original Article

1. INTRODUCTION

Aluminium and its alloys have been extensively preferred for many applications because of their excellent mechanical properties. They are the first choice of researchers and engineers because of their low density, good heat and electric conductivity, resistance to corrosion and high endurance [1]. Addition of compatible reinforcements even in small quantities would further enhance the stiffness, hardness, fatigue resistance and tribological properties of aluminum alloys in specific [2]. In the present day situation aluminum matrix composites are being used in automobile, aerospace, marine and defense industries because of superior properties [1,3] exhibited by these composites. Even with the various available methods like stir casting, pressure infiltration etc. to produce metal matrix composite Powder Metallurgy (PM) has been the most popular technique as it is simple and flexible in terms of designing the constituents [4]. The PM method greatly avoids the formation of reinforcement clusters on the matrix and reaction between the reinforcement and matrix. PM route is advantageous as higher

quantity of reinforcement can be dispersed in the matrix and also a better control of microstructure phases is achievable [5]. Also in specific by aluminum PM it is possible to produce high performance, net or nearly net to shapes of components, hence bringing down or avoiding the investment and running costs attached with complex machining operations [6]. In the recent year's researchers have used ceramic particles for producing the composites. But the major drawback with ceramics reinforced MMC's are their relatively lower toughness and toughness. Also, the relatively higher costs would make them economically unsuitable for various applications. In contrast, steels are competitively low cost, which has made them attractive in a wide range of applications [7].

In the light of above, the present investigation concentrates on to develop the composite by dispersing the mild steel particles in different proportions in duralumin matrix by employing the cold compacting approach. The composite developed is expected to provide superior mechanical properties suitable for high strength, heat and wear resistant applications.

2. METHODOLOGY

2.1. Powders Chosen for Compaction

Matrix material chosen for the present investigation is duralumin powder borrowed from Varsha bullion & elemental analab, Mumbai. The average particle size of the duralumin powder is 50 microns and are irregular in shape. The apparent density is found to be 1.2448 g/cc. The elemental composition of this material has been shown in Table 1. As seen from this table, the major alloying element in duralumin is copper with 3.9% wt. This matrix exhibits a superior blend of strength and damage resistance at higher and cryogenic temperatures [8]. Duralumin is extensively used for aircraft components like fittings, couplings, transmission shafts and for gears. The morphology of powder particles is shown in the SEM micrograph (figure 1). Micrographs were captured by SEM (EVO MA18 with Oxford EDS(X-act)) having magnification 1X and maximum 100000X.

Water atomized MS powder used as a reinforcement contains irregular particle shapes with dark grey color exhibiting high hardness with particle size in the range 40-45 microns. It is borrowed from Parshwamani metals, Mumbai. Table 2 gives the chemical components of mild steel powder.

Table 1: Chemical Components of DA Powder

Element	Si	Fe	Cu	Mn	Mg	Al
% wt.	0.142	0.192	3.9	0.5	1.22	94.0075

Table 2: Elemental Composition of Mild Steel Powder

Element	C	Mn	Cr	Mo	Si	P	S	Fe
% wt.	0.81	0.13	0.24	0.15	0.28	0.1	0.08	Bal

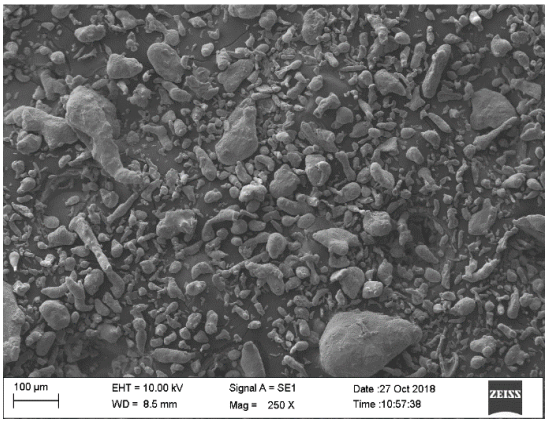

Figure 1: Micrographs Showing Morphology of Duralumin Particulates

2.2. Fabrication of Test Compacts by Cold Compacting

2.2.1. Details of Compaction Tools

The tooling used for cold compacting include simple die and punches and are as shown in figure 2. The length to diameter ratio of the die is maintained as 4 in the design. The die has been fabricated from En24 steel and the punches from En8 material. In order to induce adequate strength, the die and punches were subjected to heat treatment after machining and TIG welding operations.

Figure 2: Photographs of upperpunch, Die Block and Lower Punch

2.2.2. Mixing of Powders

The duralumin and MS_p powders are mechanically mixed in a ball milling equipment[2]. The equipment pre-loaded with steel balls is charged with two types of powders such that Ball to Charge ratio(BCR) is 5:1. This ratio is essential for obtaining the homogeneous mixture of powders [9]. The powders are milled for 60 min and at a constant speed of 200 rpm in the laboratory conditions. Because of the impact of balls on the powdery charge, the powders get cold welded and hence a homogeneous mixture is obtained. The steel balls used in milling and milling equipment are shown in figure 3.

Figure 3: Steel Balls Used in Milling (L) and the Ball Milling Equipment for Milling of Powders(R)

2.2.3. Cold Compacting of Powders

In order to apply the load on powders to compact them, UTM of 60 T capacity is used. The steadily increasing load is axially applied through the punch as shown in figure 4. The compacts of duralumin and composite (6% and 12% wt.) were produced with an applied load in the range 22-38 T. In order to avoid the seizure of compact in the die and to prevent the direct surface contact between the punch and die the surfaces of the tools are applied with a layer of zinc stearate paste. Each of the compacted specimen was removed undamaged from the die cavity by a simple ejection system that is as shown in figure 4. Some amount of minute surface cracks was observed for green composite with MS_p. The exposure of MS particles on to the hard inside die surface might have led to higher friction by breaking the lubricant and eventually MS particles might have slipped (inter particle bond breakage) from the surface leading to surface cracks. The details of compacts are tabulated in Table 3. The process of compacting of powders in UTM is as shown in figure 4 and the green compact of duralumin and that of composites are shown in photographs of figure 5.

Figure 4: (L) The Process of Compacting in UTM and (R) Ejection of Compact Specimen from the Die

Compact of Duralumin

DA+6% MS_p

DA+12% MS_p

Figure 5: Green Compacts of Composite

Table 3: Details of Green Compacts

Sl. No	Specimen Code	Duralumin (% wt.)	MS_p (% wt.)	Dimensions of Green Compact (D cm X L cm)*
1	DA	100	0	Φ2.3 X 4.2
2	DA+6%MS_p	94	6	Φ2.4 X 4.5
3	DA+12%MS_p	88	12	Φ2.4 X 4.5

*(D: Diameter & L: Length)

2.2.4. Sintering Process

The green compacts will not have sufficient strength to withstand the external load, hence in the present study they were subjected to sintering operation in a PID controlled muffle furnace. The compacts are held at 580^0C for 5 h in furnace and were let to cool down in the furnace for 18 h. The surface oxidation of compacts is prevented by loading them into furnace after the inside temperature was stabilized. The process of sintering of mainly brings about the bonding between powder particles at the contact areas and thus enhances overall strength of compact [8]. At the atomic level, sintering process provides increased bonding among atoms and diffusion of atoms and weldzonesare formed while compaction will enhance the bonding [10].

2.3. Experimental Details

2.3.1. Density and Hardness of Compacts

Density of DA and reinforced compacts was determined using a digital electronic weighing machine(0.0001 g) by adopting Archimedes' principle according to ASTM B311-08 [8,10,11]. The theoretical values of densitiesare arrived by employing rule of mixtures. The specimens of DA, DA+ 6% MS_p and DA+12%MS_p are further cut into smaller cylinders in the wire EDM machine. The process of parting is shown in figure 6 and the specimens for hardness test are as shown in figure 7. Scratches and surface defects on the sample were eliminated by thoroughly polishing the test specimens with emery papers (400, 600, 800, and 1000 grit). The hardness measurement was done at normal room temperature (30^0C) and the hardness was measured at four spots on the surface of each sample to know the average hardness. In order to measure the hardness of specimens micro Vickers hardness tester was used [2, 10,11] (Make: MATSUZAWA, Model: MMT-X7A,

Capacity: Min. 5 gf and max. 1000 gf), with diamond indenter to make indentation on the surface of specimens. A dwell time of 15 secs is maintained after the application of load 100gf. The density of compacts, porosity levels therein and their corresponding hardness values in sintered condition are tabulated in Table 4.

Figure 6: Parting Process in Wire Cut EDM

Figure 7: Specimens for Hardness Test Obtained by Parting in Wire Cut EDM

Table 4: Properties of Duralumin and Composite Compacts

Sl. No	Specimen	Theoretical Density (g/cc)	Green Density (g/cc)	Sintered Density (g/cc)	Relative Density (%)	% Porosity (Pre-Sintering)	% Porosity (Post-Sintering)	VHN of Sintered Compacts
1	DA	2.71	2.66	2.67	98.53	1.84	1.47	28
2	DA+6% MS_p	2.93	2.89	2.90	98.97	1.36	1.02	39
3	DA+12% MS_p	3.11	3.06	3.08	99.03	1.60	0.96	46

2.3.2. Aging Heat Treatment Process

The sintered compacts were made to undergo to aging treatment. The heat treatment was carried out in a PID controlled muffle furnace. The furnace temperature was initially made stable to the required temperature and then specimens were loaded to avoid the surface oxidation. Compacts are initially subjected to soaking heat treatment at 550^{O}C for span of 2 h, followed by quenching in water at ambient temperature. Hardness was measured before starting aging process and further, compacts are further aged artificially in the furnace at temperatures of 100, 150, and 200^{O}C for different intervals of time. The heat treatment curves adopted during the process cycle are depicted in figure 8.

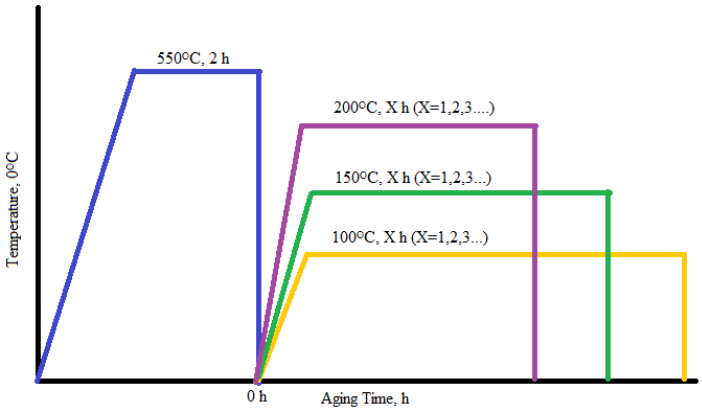

Figure 8: Heat Treatment Curves

2.3.3. Hardness of Aged Specimens

Hardness values are measured at time interval of 60 minutes, to determine the peak aging time for that specific temperature. The hardness for each interval are tabulated for all the three types of compacts carried at 100, 150 and 200^{0}C are given in Tables 5-13. Comparison of peak hardness of specimens under different conditions has been given in Table 14.

Table 5: Hardness Values of DA Specimen Aged at 100^{0}C for Different Aging Times

Sample No	0	1	2	3	4	5	6	7	8	9	10	11	12	13	14	15	16	17
Time (h) for Aging	0	1	2	3	4	5	6	7	8	9	10	11	12	13	14	15	16	17
VHN	25	25	28	30	31	33	35	37	38	40	42	47	50	56	52	48	--	--

Table 6: Hardness Values of DA+6% MS$_p$ Composite Aged at 100^{0}C for Different Aging Times

Sample No	0	1	2	3	4	5	6	7	8	9	10	11	12	13	14	15	16	17
Time (h) for Aging	0	1	2	3	4	5	6	7	8	9	10	11	12	13	14	15	16	17
VHN	35	38	42	47	51	55	60	64	75	68	65	--	--	--	--	--	--	--

Table 7: Hardness Values of DA+12% MS$_p$ Composite Aged at 100^{0}C for Different Aging Times

Sample No	0	1	2	3	4	5	6	7	8	9	10	11	12	13	14	15	16	17
Time (h) for Aging	0	1	2	3	4	5	6	7	8	9	10	11	12	13	14	15	16	17
VHN	43	46	53	62	84	73	70	--	--	--	--	--	--	--	--	--	--	--

Table 8: Hardness Values of DA Specimen Aged at 150^{0}C for Different Aging Times

Sample No	0	1	2	3	4	5	6	7	8	9	10	11	12	13	14	15	16	17
Time (h) for Aging	0	1	2	3	4	5	6	7	8	9	10	11	12	13	14	15	16	17
VHN	25	27	29	30	32	34	36	38	40	42	44	48	49	45	43	--	--	--

Table 9: Hardness Values of DA+6% MS$_p$ Composite Aged at 150^{0}C for Different Aging Times

Sample No	0	1	2	3	4	5	6	7	8	9	10	11	12	13	14	15	16	17
Time (h) for Aging	0	1	2	3	4	5	6	7	8	9	10	11	12	13	14	15	16	17
VHN	36	41	43	45	50	51	63	50	48	--	--	--	--	--	--	--	--	--

Table 10: Hardness Values of DA+12% MS_p Composite Aged at 150^{0}C for Different Aging Times

Sample No	0	1	2	3	4	5	6	7	8	9	10	11	12	13	14	15	16	17
Time (h) for Aging	0	1	2	3	4	5	6	7	8	9	10	11	12	13	14	15	16	17
VHN	44	48	52	68	56	51	49	--	--	--	--	--	--	--	--	--	--	--

Table 11: Hardness Values of DA Specimen Aged at 200^{0}C for Different Aging Times

Sample No	0	1	2	3	4	5	6	7	8	9	10	11	12	13	14	15	16	17
Time (h) for Aging	0	1	2	3	4	5	6	7	8	9	10	11	12	13	14	15	16	17
VHN	26	28	30	31	33	35	38	39	41	42	43	41	39	---	---	---	---	---

Table 12: Hardness Values of DA+6% MS_p Composite Aged at 200^{0}C for Different Aging Times

Sample No	0	1	2	3	4	5	6	7	8	9	10	11	12	13	14	15	16	17
Time (h) for aging	0	1	2	3	4	5	6	7	8	9	10	11	12	13	14	15	16	17
VHN	37	42	44	47	49	58	45	44	--	--	--	--	--	--	--	--	--	--

Table 13: Hardness Values of DA+12% MS_p Composite Aged at 200^{0}C for Different Aging Times

Sample No	0	1	2	3	4	5	6	7	8	9	10	11	12	13	14	15	16	17
Time (h) for Aging	0	1	2	3	4	5	6	7	8	9	10	11	12	13	14	15	16	17
VHN	44	48	65	50	48	--	--	--	--	--	--	--	--	--	--	--	--	--

Table 14: Comparative Tabulation of Peak Hardness of Specimens under Different Conditions

Condition	Duralumin(DA)	DA+6% MS_p	DA+12% MS_p
Sintered	28	35	42
Peak aged at 100^{0}C	56	75	84
Peak aged at 150^{0}C	49	63	68
Peak aged at 200^{0}C	43	58	65

2.3.4. Tension Test

The tensile test specimens were fabricated from the cylindrical peak hardened compacts as per E8/E8M-13a standard [12]. The tensile test was carried out in a Tensometer which was computer integrated to generate the on line plot of load-vs-extension. The results of tension test are tabulated in Table 15.

Table 15: Tensile Properties of Duralumin and Composite Compacts

Sl. No	Specimen	Ultimate Tensile Strength (MPa)			
		As Sintered	100^{0}C	150^{0}C	200^{0}C
1	DA	90	135	121	110
2	DA+6%MS_p	103	193	162	151
3	DA+12%MS_p	112	213	174	166

3. RESULTS AND DISCUSSIONS

3.1. Density of Compacted Specimens

As the quantity of MS_p is increased, an increase in the density of the composites is noticed. This behavior could be because of relatively high packing factor of MS_p, increased concentration within the duralumin resulting in increase of the density of the composites. This behavior is furthermore increased by an effective fusion of MS_p while sintering to form

a coherent body with the duralumin. This indicates a good vitrification of the composites while the process of sintering[13].

Figure 9 depicts the variation of density of composite compacts with increasing amount of MS_p. This behavior is increased by the proper fusion of MS_p while sintering with the matrix to form a coherent phase. Relative density is calculated by using the relation, Relative density=sintered density/theoretical density [12] and its variation is depicted in figure 10. A decrease in the level of porosity is observed as the amount of MS_p is increased (figure 11) and is due to strong interfacial bonding between the particles during sintering at elevated temperature. Lower porosity levels basically provide composite materials with improved mechanical properties. As a result of lower porosity in the compacts, they definitely exhibit superior strengths, high load carrying ability, and good corrosion resistance. The variation of porosity of composites in the present investigation matches with the observations noticed by investigators to develop brake pads[14].

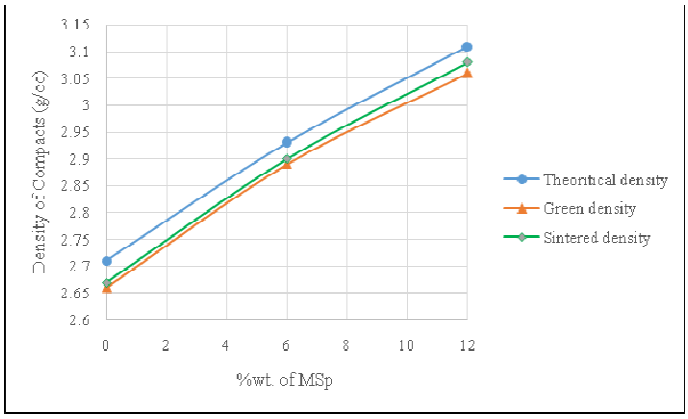

Figure 9: Variation of Density of Compacts with the Amount of MS Particles in the Matrix

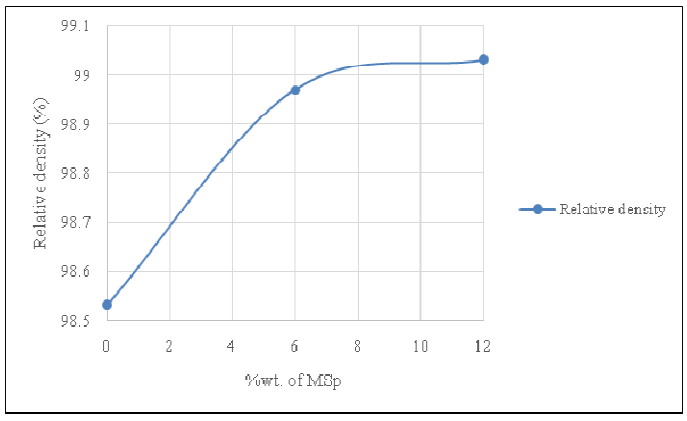

Figure 10: Variation of Relative Density of Compacts with the Amount of MS Particles

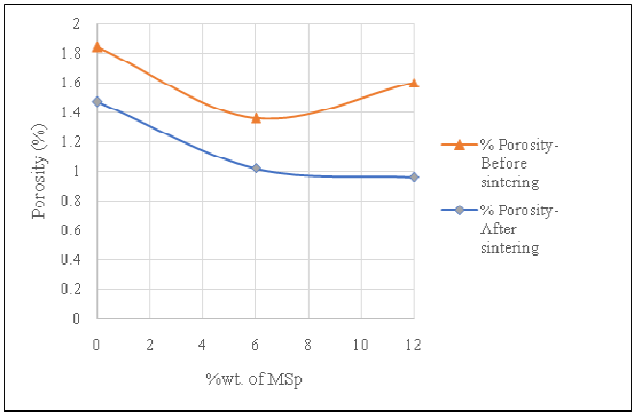

Figure 11: Variation of Porosity Level in Compacts with the Amount of MS Particles

3.2 Microstructure Study on Sintered Compacts

As seen from the SEM images shown in figure 12, there is fairly homogeneous dispersion of mild steel particles in the entire duralumin matrix with no surface porosity or cracks. Also, it appears to be a fair bondage among DA and MS_p that could certainly result in the improved load transfer from the matrix to reinforcements in the composites. As observed from the micrographs, there is no clustering of MS_p in DA, which is very common in the liquid state processing techniques. Figure 13 depicts the EDAX spectrum taken on sintered composite compact which confirms the elemental composition.

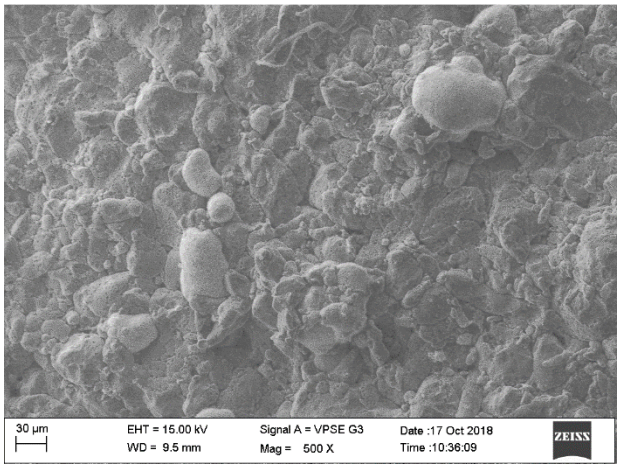

Figure 12: SEM Micrograph of Sintered Composite Compact Confirming the Uniform Distribution of MS_p (12% wt.) in the Matrix Phase

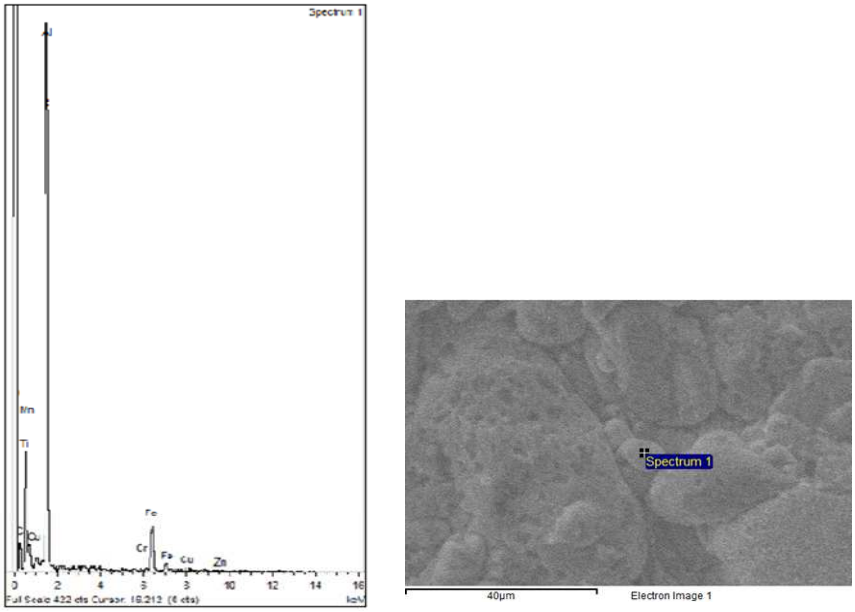

Figure 13: EDAX Spectrum Taken on Sintered Composite Compact Confirming the Presence of MS_p in the Matrix Phase

3.3. Hardness in Sintered and Aged Condition

As can be seen in figure 14, as the amount of reinforcement is increased in matrix the hardness of composite will also increase. The enhancement of hardness could be because of higher quantity of MS_p and also higher amount of intermetallic phases appearing with steel particle addition during heat treatment. Earlier studies have noticed that iron enhances the strength in compression and composite hardness. The strengthening mechanism isbecause of refinement of grains of DA matrix, the homogeneous dispersion reinforced particles, as well as the appearance of $Al_{13}Fe_4$ intermetallic compound [15].

Both DA and DA-6% and 12% wt. aged samples are subjected to hardness measurement (VHN). Variation of hardness as a function of temperature of aging and duration for the above composites are depicted in figures 15-20. Hardness is found to increase gradually with time for both the DA and its composites. It reaches peak hardness value followed by over-aging that results in decrease of hardness [16]. The hardness increases with increase in amount of mild steel particulates. The increase in hardness is because of hard reinforcement particles that positively contributes to the hardness of composites [17]. Since matrix is strong age hardenable alloy, it is expected that mild steel reinforced DA alloy composites may be very sensitive to age hardening regardless of temperature of aging. Among all the aging temperatures, aging at 100°C for both base alloy and its composites show higher peak hardness values although the time intervals for achieving peak aging are considerably higher. Artificial aging at lower temperature (100°C) pays to the enhanced hardness due to escalation in the quantity of intermediate zones throughout precipitation, higher amount of fine intermetallics and reduced interparticle distances. The hardness reduces after peak aged state, could be because of increased size of intermetallic precipitates that appear while aging process and existence of incoherency between matrix and intermetallics termed as over-aging [18]. Higher temperatures (150 and 200°C) accelerate the aging rate because of increased diffusion rate in the matrix. Higher the temperature of aging, lower will be the duration required to achieve peak hardness [16]. Comparison of variation of peak hardness with quantity of mild steel particles for sintered condition and for different aging temperatures is shown in figure 21.

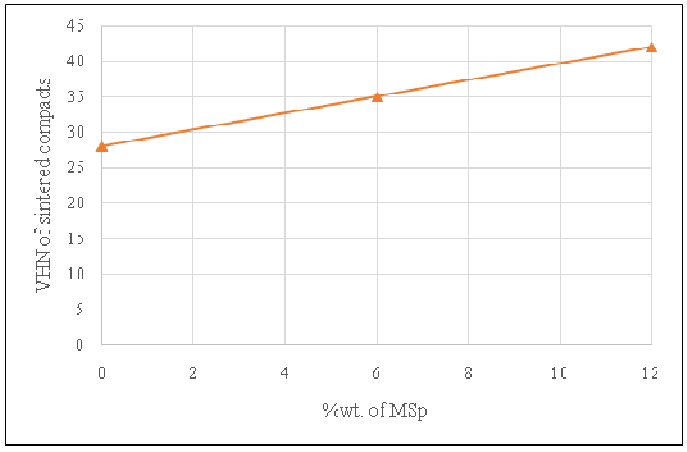

Figure 14: Variation of VHN of Compacts with the Amount of MS Particles

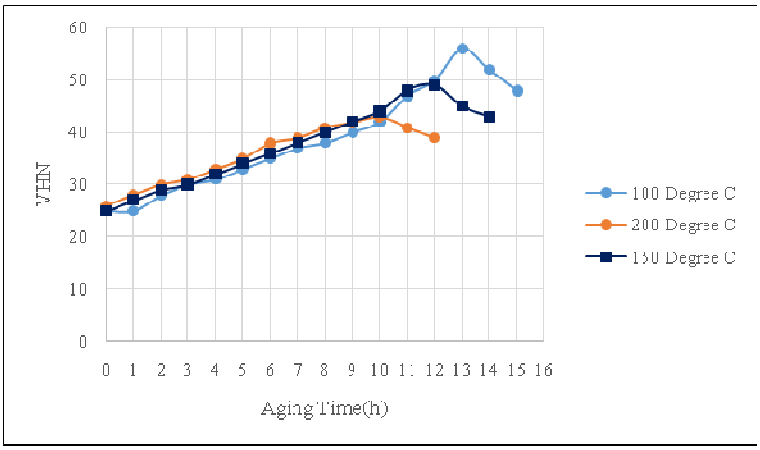

Figure 15: Variation in Hardness with Aging Time for Duralumin Compact

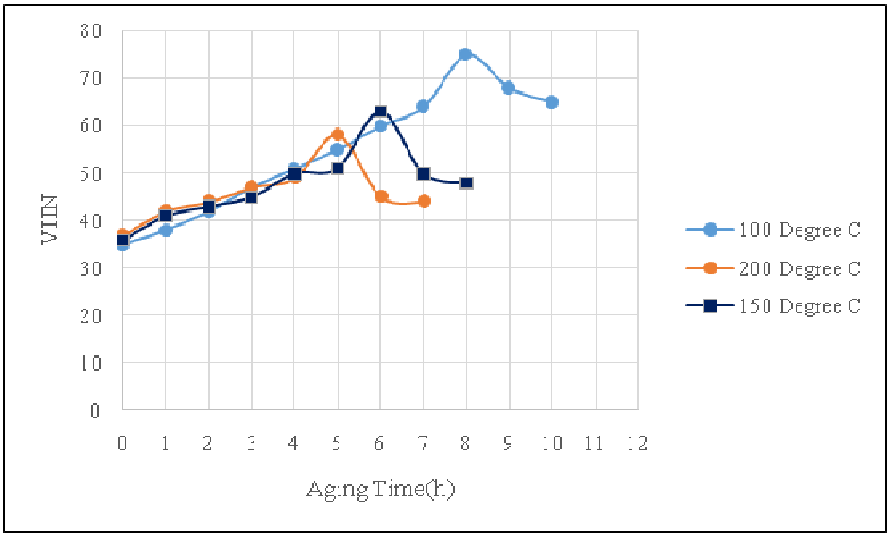

Figure 16: Variation in Hardness as a Function Aging Time for DA+6% MS_p Compact

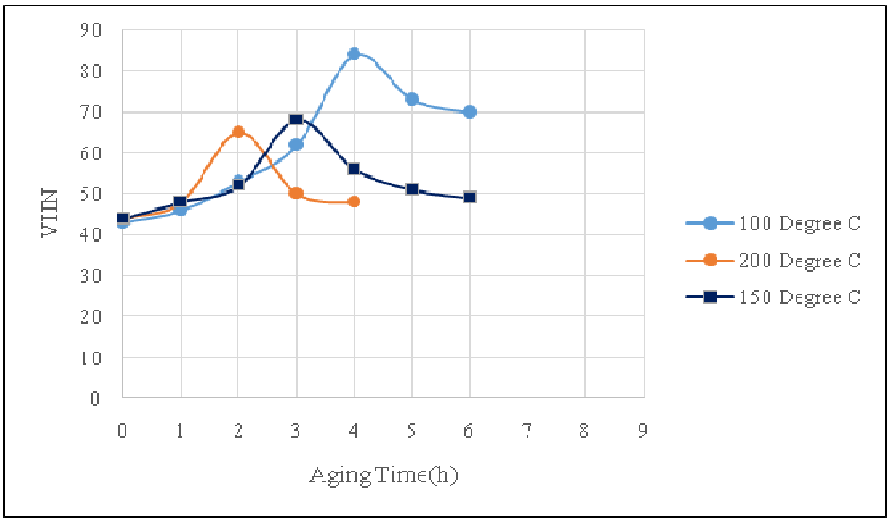

Figure 17: Variation in Hardness as a Function Aging Time for DA+12% MS_p Compact

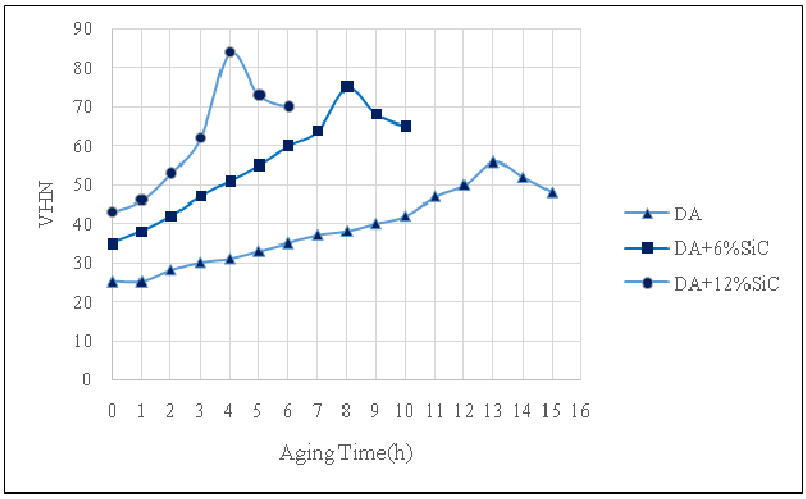

Figure 18: Comparison of Variation of Hardness as a Function of Aging Time for all Compacts Aged at 1000C

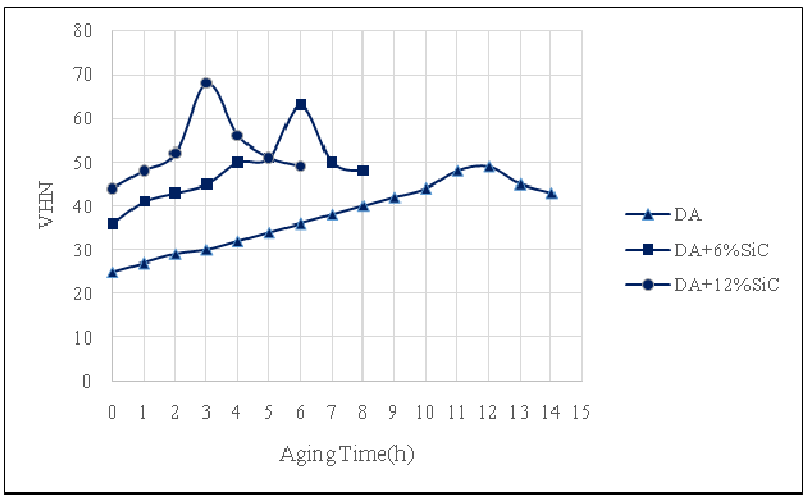

Figure 19: Comparison of Variation of Hardness as a Function of Aging Time For Compacts Aged at 1500C

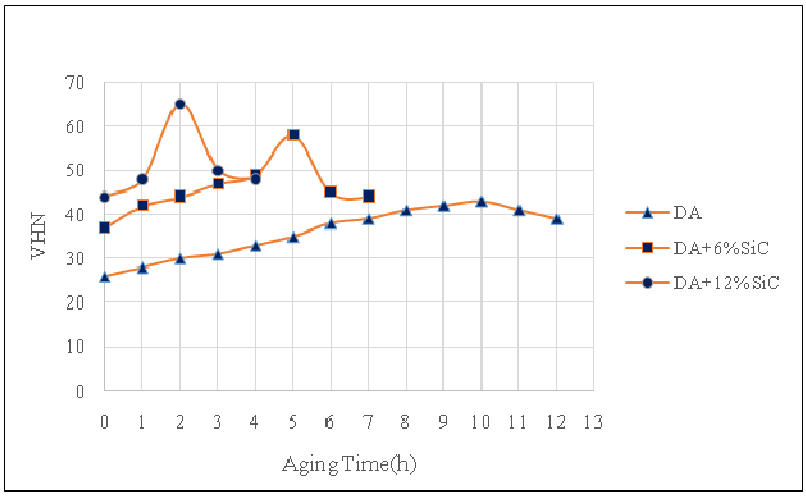

Figure 20: Comparison of Variation of Hardness as a Function of Aging Time for Compacts Aged at 2000C

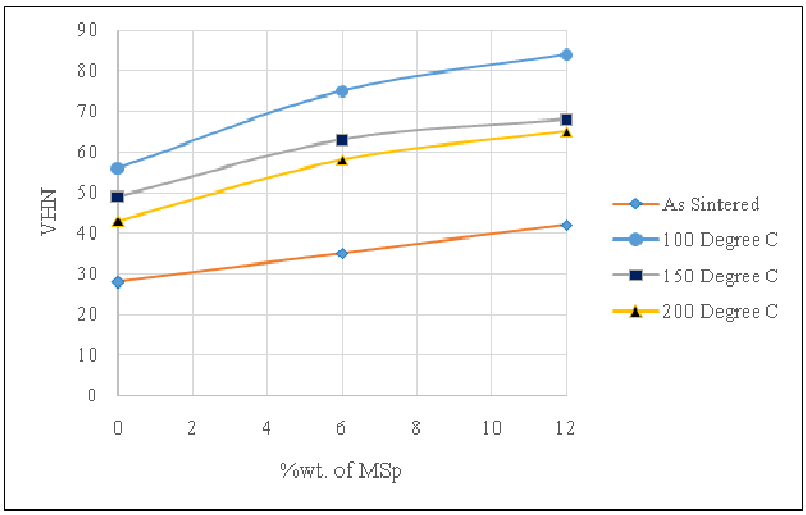

Figure 21: Comparison of Variation of Peak Hardness with Amount of MS_p for Sintered Condition and for Different Aging Temperatures of Compacts

3.4. Tensile Test

The specimens are observed to have undergone primarily the ductile fracture, with cup and cone shape formed on the fractured halves of the samples. Tension test is performed on DA and peak aged samples. Figure 22 shows the comparison of variation of UTS with quantity of MS_p for sintered condition and for different aging temperatures of compacts. Uniform distribution of the reinforcement particles is an important requirement for various high performance engineering applications. A homogeneous distribution of individual and hybrid reinforcements is essential to improve the composites mechanical properties achieved by strong interfacial bonding, which contributes for effective load transfer and distribution from the matrix to the reinforcements exhibiting enhanced elastic modulus and strength. The improvement in tensile strength by the presence of hard secondary phases on soft matrix leads to alloy strengthening, which also helps to decrease grain size of the matrix resulting further improvement of mechanical properties [19, 20]. Higher particle concentration and lower aging temperature result in a higher density of dislocations and particle interaction dislocations. When load is applied, the presence of the hard particles and intermetallics contribute to dislocation pileup, increasing back

stress, and work hardening the matrix due to restricted plastic flow in the ductile matrix. The synergetic effect of dislocation interaction with the reinforcement, intermetallic and grain boundary provides a positive contribution to alloy strengthening [21, 22].

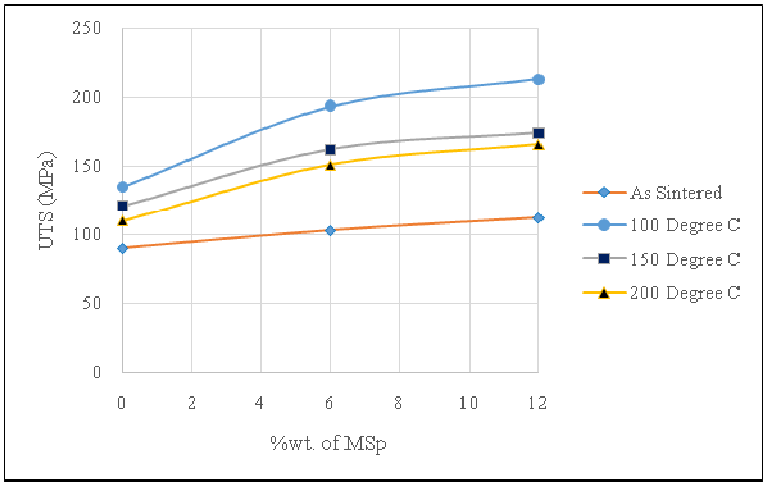

Figure 22: Comparison of Variation of UTS with Amount of MS_p for Sintered Condition and for Different Aging Temperatures of Compacts

4. CONCLUSIONS

In the present investigation the compacts of duralumin and the duralumin based mild steel particles reinforced composites were successfully fabricated by cold compacting the powders and the sintered composite specimens showed a homogeneous dispersion of the MS_p in DA matrix. An increase in the densities of the composites was noticed as the amount of mild steel particulates is increased and this may be due to a relatively higher packing factor of MS_p. The porosity level is observed to have decreased with increased amount of MS_p and this behavior may be because of strong bond at the interface among particles through elevated temperature sintering. Because of accelerated aging rate at higher temperatures (150 and 200^{0}C as compared to 100^{0}C) the time required to attain peak hardness was observed to be less comparatively. Specimen peak aged at 100^{0}C displayed a good improvement in UTS than the counterparts peak aged at 150 and 200^{0}C.

REFERENCES

1. *Halil Karakoça, Şener Karabulut and Ramazan Çıtak, Study on mechanical and ballistic performances of boron carbide reinforced Al 6061 aluminum alloy produced by powder metallurgy, Composites Part B 148 (2018) 68–80.*
2. *Prashantha Kumar H.G and Anthony Xavior .M, Assessment of mechanical and tribological properties of Al 2024-SiC-Graphene hybrid composites, Procedia Engineering 174 (2017) 992 – 999.*
3. *Naiqin Zhao, Philip Nash and Xianjin Yang, The effect of mechanical alloying on SiC distribution and the properties of 6061 aluminum composite, Journal of Materials Processing Technology 170 (2005) 586–592.*
4. *X.Z. Zhang, T.J. Chen and Y.H. Qin, Effects of solution treatment on tensile properties and strengthening mechanisms of SiCp/6061Al composites fabricated by powder thixoforming, Materials and Design 99 (2016) 182–192.*
5. *S. Sivasankaran , K. Sivaprasad , R. Narayanasamy and Vijay Kumar Iyer, An investigation on flowability and compressibility of AA 6061100−x-x wt.% TiO2 micro and nanocomposite powder prepared by blending and mechanical alloying, Powder Technology 201 (2010) 70–82.*

6. *Ikhwan, M. K., Azis, R. S., Hashim, M., Holland, D., Zulkimi, M., Zakaria, A., & Hassan, J. (2014). Yttrium aluminum monoclinic (YAM) synthesized by high energy ball milling. Int. J. Res. Appl. Nat. Soc. Sci, 2(2), 85-90.*
7. *M.A. Jabbari Taleghani, E.M. Ruiz Navas and J.M. Torralba Microstructural and mechanical characterisation of 7075 aluminium alloy consolidated from a premixed powder by cold compaction and hot extrusion, Materials and Design 55 (2014) 674–682.*
8. *Catherine Kuforiji and Michel Nganbe. Powder metallurgy fabrication, characterisation and wear assessment of SS316L-Al2O3 composites, Tribology International 130 (2019) 339–351.*
9. *P. Ravindran , K. Manisekar , P. Rathika and P. Narayanasamy, Tribological properties of powder metallurgy – Processed aluminium self lubricating hybrid composites with SiC additions, Materials and Design 45 (2013) 561–570.*
10. *Anil Kumar Bodukuria, K. Eswaraiahb, Katla Rajendara and V. Sampath, Fabrication of Al—SiC—B4C metal matrix composite by powder metallurgy technique and evaluating mechanical properties, Perspectives in Science (2016) 8, 428—431.*
11. *Muhammad Irfan Ab Kadira, Mohammad Sukri Mustapa, Noradila Abdul Latifa and Ahmed Sahib Mahdia, Microstructural Analysis and Mechanical Properties of Direct Recycling Aluminium Chips AA6061/Al Powder Fabricated by Uniaxial Cold Compaction Technique, Procedia Engineering 184 (2017) 687 – 694.*
12. *H.M. Zakaria (2014). Microstructural and corrosion behavior of Al/SiC metal matrix composites, Ain Shams Engineering Journal, 5, 831–838.*
13. *Mahdi Dehestani, Erik Adolfsson and Lia A. Stanciu, Mechanical properties and corrosion behavior of powder metallurgy iron-hydroxyapatite composites for biodegradable implant applications, Materials and Design 109 (2016) 556–569.*
14. *Irfan, O. M. Influence Of Specimen Geometry And Lubrication Conditions On The Compression behavior Of Aa6066 Aluminum Alloy.*
15. *Stephen I. Durowayea, Olatunde I. Sekunowoa, Abdulganiyu I. Lawala and Olusola E. Ojo. Development and characterisation of iron mill scale particle reinforced ceramic matrix composite. Journal of Taibah University for Science 11, 634–644 (2017)*
16. *O.I. Sekunowo, S.I. Durowaye and G.I. Lawal. Synthesis and characterisation of iron millscale particles reinforced ceramic matrix composite. Journal of King Saud University – Engineering Sciences 31, 78–85 (2019)*
17. *Kenneth Kanayo Alanemea, Adetomilola Victoria Fajemisina and Nthabiseng Beauty Maledi. Development of aluminium-based composites reinforced with steel and graphite particles: structural, mechanical and wear characterization, journal of materials research technology (2018). Article in press.*
18. *Rajasekaran, S., Udayashankar, N. K and Nayak, J, T4 and T6 treatment of 6061 Al-15 Vol.% SiC composite. ISRN Materials Science (2012) 1-5.*
19. *Kumar, G. V., Rao, C. S. P., Selvaraj, N., and Bhagyashekar, M. S, Studies on Al6061-SiC and Al7075-Al2O3 metal matrix composites. Journal of Minerals and Materials Characterization and Engineering, 9(1) (2010) pp.43-55.*
20. *Rafiq, A. S., Abdullah, H. A., and Al-Belushi, K. R, Influence of aging parameters on the mechanical properties of 6063 aluminium alloy. Journal of Materials Processing Technology, 102(1) (2000) pp.234-240.*
21. *Ibrahim, M. F., Ammar, H. R., Samuel, A. M., Soliman, M. S., Almajid, A., and Samuel, F. H, Mechanical properties and fracture of Al–15 vol.% B4C based metal matrix composites. International Journal of Cast Metals Research, 27(1) (2014) pp.7-14.*
22. *Auradi, V., Rajesh, G. L., and Kori, S. A, Processing of B4C particulate reinforced 6061aluminum matrix composites by melt stirring involving two-step addition. Procedia Materials Science, 6, (2014) pp.1068-1076.*

23. *Milan, M. T. and Bowen, P, Tensile and fracture toughness properties of SiCp reinforced Al alloys: Effects of particle size, particle volume fraction, and matrix strength. Journal of Materials Engineering and Performance, 13(6), (2004) pp.775-783.*
24. *Ahn, H. K., & Yu, C. H. (2001). Effect of SiC volume fraction on the age-hardening behavior in SiC particulate-reinforced 6061 aluminum alloy composites. Metals and Materials International, 7(1),(2001) pp.1-7.*
25. *en.wikipedia.org/wiki/Transmission_(mechanics).*